Antifibrotic efficacy of nintedanib in a cellular model of systemic sclerosis-associated interstitial lung disease

I. Atanelishvili[1], T. Akter[1], A. Noguchi[1,2], O. Vuyiv[1], L. Wollin[3], R.M. Silver[1], G.S. Bogatkevich[1]

[1]*Division of Rheumatology and Immunology, Department of Medicine, Medical University of South Carolina, Charleston, SC, USA;*
[2]*Division of Rheumatology, Endocrinology and Nephrology, Hokkaido University Graduate School of Medicine, Sapporo, Japan;*
[3]*Boehringer Ingelheim GmbH & Co. KG, Biberach, Germany.*

Ilia Atanelishvili, MS
Tanjina Akter, PhD
Atsushi Noguchi, MD, PhD
Olha Vuyiv
Lutz Wollin, PhD
Richard M. Silver, MD
Galina S. Bogatkevich, MD, PhD

Please address correspondence to:
Dr Galina S. Bogatkevich, 96 Jonathan Lucas Street, Suite 904, Medical University of South Carolina, Charleston, SC 29425, USA.
E-mail: bogatkev@musc.edu

Received on March 20, 2019; accepted in revised form on September 2, 2019.

Clin Exp Rheumatol 2019; 37 (Suppl. 119): S115-S124.

Key words: systemic sclerosis, interstitial lung disease, nintedanib, fibroblast

Funding: This work was supported in part by a grant from Boehringer Ingelheim International GmbH (to G.S. Bogatkevich).

Competing interests: L. Wollin is an employee of Boehringer Ingelheim (inventor of nintedanib). R.M. Silver has received research funding and has served as a consultant for Boehringer Ingelheim. The other co-authors have declared no competing interests.

ABSTRACT

Objective. *Nintedanib is approved for the treatment of idiopathic pulmonary fibrosis (IPF) and was demonstrated to slow disease progression in patients with IPF by reducing decline in forced vital capacity by 50%. Recently, nintedanib has been reported to exert anti-fibrotic activity on systemic sclerosis (scleroderma, SSc) skin fibroblasts and to diminish skin and lung fibrosis in mouse models. The goal of the present study was to determine the effects of nintedanib on a cellular model of SSc-associated interstitial lung disease (ILD).*

Methods. *Study was performed using lung fibroblasts (LF) isolated from five patients with SSc-ILD and from three control subjects.*

Results. *Nintedanib inhibited LF proliferation and migration in a concentration- and time-dependent manner. The proliferation rate of LF stimulated with PDGF in the presence of nintedanib was reduced 1.9-fold within 24 h as compared to cells stimulated with PDGF alone. Migration of SSc-ILD LF incubated with 100 nM nintedanib was reduced from 62.8±12.5% to 39.1±9.0% in the presence of PDGF and from 38.2±7.9% to 26.6±7.2% in serum-free medium. Nintedanib attenuated PDGF-induced Ca^{2+} efflux, reduced α-SMA promoter activity and α-SMA protein expression. Furthermore, nintedanib blocked PDGF-induced differentiation of normal LF to myofibroblasts, reduced production of collagen and fibronectin, and decreased contractility of SSc-ILD LF in both floating and fixed collagen gels.*

Conclusion. *Our data demonstrate significant antifibrotic efficacy of nintedanib in SSc-ILD LF suggesting that nintedanib has the potential not only to prevent but also to reverse the increased activity of LF consequently attenuating excessive lung fibrosis observed in SSc-ILD.*

Introduction

Pulmonary fibrosis is the end-stage of many chronic lung diseases including systemic sclerosis (scleroderma, SSc) associated interstitial lung disease (SSc-ILD) and idiopathic pulmonary fibrosis (IPF). The conceptual process of fibrogenesis in pulmonary fibrosis involves the presence of alveolar damage, followed by the release of fibrogenic factors, induction of myofibroblasts, accumulation and excessive deposition of extracellular matrix (ECM) proteins, the net result of which is severe lung dysfunction and mortality. *In vitro* studies have consistently shown that fibroblasts isolated from SSc patients retain their pro-fibrotic phenotype for several passages in cell culture and can be used as a model system for understanding the nature of persistent fibrosis (1, 2).

Platelet-derived growth factor (PDGF) is a major mitogen for mesenchymal cells and the strongest identified proliferative stimulus for fibroblasts (3). In the human lung, PDGF is produced mainly by alveolar macrophages and epithelial cells (3, 4). Five different isoforms of PDGF ligands (PDGF-AA, PDGF-BB, PDGF-CC, PDGF-DD, PDGF-AB) and two PDGF receptor (R) isotypes (PDGFR-α and PDGFR-β) with three different PDGFR dimers (PDGFR-α/α, PDGFR-α/β and PDGFR-β/β) have been described (3). PDGF ligands are elevated in epithelial cells and alveolar macrophages of IPF patients (5) and in bronchoalveolar lavage fluid (BALF) from scleroderma patients (6).

Nintedanib interferes with the ATP-binding pocket of several tyrosine kinase receptors including PDGFR, fibroblast growth factor receptors (FGFR), and vascular endothelial growth factor (VEGFR) (7, 8). Nintedanib was demonstrated to inhibit proliferation and migration and to reduce smooth muscle α-actin (α-SMA) and ECM proteins in

lung fibroblasts (LF) from IPF patients (9-12). Recently, nintedanib was also reported to inhibit the endogenous and cytokine-induced activation of scleroderma skin fibroblasts and to diminish skin fibrosis in several SSc mouse models (13).

The present study was designed to investigate effects of nintedanib on LF isolated from SSc-ILD patients or control cells treated with profibrotic agents, such as TGFβ and PDGF.

Materials and methods

Materials

Nintedanib esilate (powder) was obtained from Boehringer Ingelheim Pharma GmbH & Co KG, Biberach, Germany (clinical grade); nintedanib was solubilised in water to receive 100 mM stock solution and stored at -20°C in 100 µl aliquots covered by aluminum foil. PDGF-BB and TGFβ1 were purchased from R&D Systems (Minneapolis, MN, USA); pirfenidone, anti-α-SMA and anti-β-actin antibodies were obtained from Sigma-Aldrich (St. Louis, MO, USA); type I collagen from rat tail tendon was purchased from BD Bioscience (Bedford, MA, USA), anti-type I collagen antibody was purchased from SouthernBiotech (Birmingham, AL, USA). 4'-6-Diamidino-2-phenylindole (DAPI) and BCA™ protein assay were obtained from Pierce (Rockford, IL, USA). Anti-fibronectin antibody and FITC-conjugated goat anti-mouse antibody were obtained from Santa Cruz Biotechnology (Santa Cruz, CA, USA); Quick Cell Proliferation Assay was acquired from BioVision Research Products (Mountain View, CA, USA).

Cell culture

LF were derived from de-identified lung tissues obtained at autopsy from five SSc-ILD patients who fulfilled the 2013 ACR/EULAR classification criteria for SSc (14) and had clinical and radiographic evidence of pulmonary fibrosis. The diagnosis of SSc-ILD was confirmed by histological examination of postmortem lung tissue. Normal lung fibroblasts were isolated from three age-matched individuals who died from non-pulmonary causes. Lung tissue was diced (0.5 x 0.5 mm pieces) and cultured in Dulbecco's modified Eagle's medium (DMEM; Gibco, Grand Island, NY, USA) supplemented with 10% fetal bovine serum (FBS), 2 mM l-glutamine, 50 µg/ml of gentamicin sulfate, and 5 µg/ml of amphotericin B at 37°C in 10% CO_2. Medium was changed every three days to remove dead and non-attached cells until fibroblasts reached confluence. Monolayer cultures were maintained in the same medium. LF were used between second and fourth passages in all experiments. Viability of all cells used in the study was confirmed by ApoSENSOR™ cell viability assay or trypan blue cell counting assay as previously described (15).

RNA isolation and RT-PCR analysis

Cells were cultured in the absence or presence of PDGF-BB and nintedanib in serum-free medium for 24 hours and subjected to total RNA extraction with the RNA Isolation Kit from Qiagen (Valencia, CA, USA) according to manufacturer's recommendations. RNA purity and amount isolated was determined by spectrophotometric analysis. Reverse transcription was performed with the SuperScript II First-Strand Synthesis Kit from Invitrogen (Carlsbad, CA, USA) and RT-PCR was performed with SYBR Green PCR Master Mix Kit from Bio-Rad (Hercules, CA, USA). PCR primers, synthesised by Eurofins Genomics (Louisville, KY, USA) were as follows: PDGFR-β forward GCTGTTGCTGTCTCTCCTGT, PDGFR- β reverse CAGGTCAGAACGAAGGTGCT; PDGFR-α forward GCCTAATCCTCTGCCAGCTT, PDGFR-α reverse ACTGCCA GCTCACTTCACTC; collagen type I forward CCAGAAGAACTGGTACATCAGCA, collagen type I reverse CGCCATACTCGAACTGGAAT; fibronectin forward CTGACAGCTCATCCGTGGTT, fibronectin reverse CTGAGCTGGTCTGCTTGTCA; Glyceraldehyde-3-phosphate dehydrogenase (GAPDH) forward GGTCTCCTCTGACTTCAACA, GAPDH reverse AGCCAAATTCGTTGTCATAC. RT-PCR was performed on a Bio-Rad MyIQ single color Real-Time PCR detection system under the following conditions: 95°C for 3 min, followed by 35 cycles at 95°C for 30 sec and 60°C for 1 min. Relative differential expression of genes was calculated using the method described by Pfaffl (16) with GAPDH serving as a housekeeping gene. Product size of the gene-specific transcripts was routinely confirmed by agarose gel.

Measurements of the intracellular calcium (Ca^{2+}) level

Cells were seeded (~30,000 cell/150 µl/well) in 96-well, clear-bottomed black microplates (Corning Costar Corp., Cambridge, MA, USA) 18 h before the experiments. On the day of assay, cells were washed with PBS, serum starved for 3 h, and incubated with or without nintedanib (100 nM) for 30 min followed by incubation in the dye-loading HEPES buffer for another 2 h. During the data run, cells were challenged with or without PDGF-BB, and fluorescence signals were recorded simultaneously for 30 min with one-second interval using the fluorometric imaging plate reader (FLIPR) system (Molecular Devices Corp., Sunnyvale, CA, USA) equipped with an electron multiplying charge-coupled device camera and Molecular Devices ScreenWorks® system control software.

Quick cell proliferation assay and cell counting

LF (10^4/well) were cultured in 96-well plates in a final volume of 100 µl/well DMEM in the absence or presence of PDGF-BB and nintedanib. After 24 hours of incubation, 10 µl/well tetrazolium salt WST-1 in Electro Coupling Solution (ECS) was added, and cells were incubated for another two hours under standard culture conditions. Plates were then placed for 1 minute on a shaker, and the optical density (OD) of each well was determined using a micro plate reader set to 450 nm.

For cell counts lung fibroblasts were detached from six-well plates, and a 0.5 ml aliquot of cell suspension was diluted in 9.5 ml of Isoton II solution for counting in Z1 Coulter particle counter (Coulter Electronics, Hialeah, FL, USA). The number of cells per dish was calculated based on a dilution factor that was identical for all groups.

Preparation of cell extracts and immunoblotting

Normal and SSc LF on 100-mm dishes were washed with ice-cold PBS and lysed with ice-cold lysis buffer (10 mM Tris, 10 mM EDTA, 1% Nonidet P-40, 0.5% deoxycholate, 0.1% SDS, pH=7.4). Protein concentration was determined by BCA™ protein assay in accordance with the manufacturer's instruction. For each sample, 40 μg of protein was denatured, subjected to SDS-polyacrylamide gel electrophoresis and analysed by immunoblotting with appropriate antibodies. The immunoblots were then stripped and reblotted with anti-β-actin antibody as a loading control.

Cell migration "scratch" assay

LF were cultured to form a monolayer on 6-well plates coated with fibronectin (10 μg/ml). Cells were serum deprived overnight and then mechanically "wounded" by scraping with a Fisherbrand ready-tip (size 1-200 μl). Cell monolayers were washed twice with PBS and incubated with or without nintedanib, PDGF, and cell proliferation inhibitor 5-Fluorouracil (Sigma, Saint Louis, MO, USA). After 6 hours of incubation fibroblasts were washed with PBS and stained by Diff-Quick Solution. Pictures were taken at 2.5 X magnification. Migration rate was calculated by counting the cells that cross into the "scratch" area and presented as a percentage of total cells on identical "non-scratch" area (100%).

Luciferase assay

LF were cultured in 24-well plates, transfected with human α-SMA promoter luciferase reporter construct (generously provided by Dr. Gerard Elberg, University of Oklahoma Health Sciences Center, USA) using Effectene Transfection Reagent. In order to standardise for transfection efficiency, cells were co-transfected with green fluorescent protein (GFP) plasmid. The cells were incubated with or without PDGF, TGFβ1, and nintedanib for 24 h and lysed in Passive Lysis Buffer according to the Promega luciferase assay system protocol. The luciferase activity of the cell lysates was measured with luciferase substrate using a luminometer. Data are expressed as relative firefly luciferase signal normalised by the GFP signal for each individual analysis. Each sample was analysed in triplicate.

Collagen gel contraction assays

Collagen lattices were prepared with type I collagen from rat tail tendon adjusted to a final value of 2.5 mg/ml with 0.01% acetic acid. LF at a concentration of 2.5 x 10^5 cells/ml were suspended in collagen (1.25 mg/ml of collagen) and aliquoted into 24 well plates (300 μl/well). Collagen lattices were polymerised for 45 minutes in a humidified 10% CO_2 atmosphere at 37°C followed by incubation with DMEM containing 10% FBS for 4 hours. For floating gel experiments, polymerised gels were gently released from the underlying culture dish followed by overnight incubation in serum-free medium and treatment with or without nintedanib and PDGF. For fixed gel experiments, gels remained attached to tissue culture dishes for the duration of the experiment. To determine the degree of collagen gel contraction, pictures were taken after 24 and 48 hours with a digital camera. Measurement of the diameter of each gel in millimeters (mm) was recorded as the average values of the major and minor axes. Calculation of gel contraction was presented as difference between diameters of wells and contracted gels. In some experiments, collagen gels were collected, digested with collagenase and analysed by Western blot using anti-SM-α actin and β-actin antibodies.

α-SMA expression and organisation assay

Human LF were cultured to subconfluence on glass slides in DMEM containing 10% FBS, after which medium was changed to serum-free medium. Cells were stimulated for 24 hours with or without PDGF in the presence or absence of nintedanib. After incubation, cells were washed with cold PBS, fixed in methanol at -20°C for 4 min and washed with cold PBS twice followed by incubation with α-SMA antibody (1:500) for 1 hour at room temperature. Cells were washed three times with cold PBS, incubated with Alexa Fluor 488 anti-mouse IgG (1:200) and DAPI (1:10 000) for 1 h at room temperature, then washed with cold PBS, air-dried, covered and sealed. Images were acquired with an Olympus IX71 fluorescence microscope equipped with objective x60/1.42 and Olympus Slidebook 4.1 software.

Statistical analysis

Statistical analyses were performed with KaleidaGraph 4.0 (Synergy Software, Reading, PA, USA) and GraphPad Prism 7 statistical software (GraphPad Software, Inc. La Jolla, CA, USA). All data were analysed using ANOVA with Tukey HSD post-hoc testing or paired t-test. The results were considered significant if $p<0.05$.

Human samples statement

The research presented in this report is qualified as "Not Human Subjects Research" in accordance with the Medical University of South Carolina Institutional Review Board (MUSC IRB). All de-identified specimens were received from the MUSC Multidisciplinary Clinical Research Center under the research proposal Pro00021985.

Results

Characterisation of PDGF receptors in scleroderma lung fibroblasts

LF express both PDGFRs, PDGFRα and PDGFRβ (3, 17). To determine which of PDGFR dominates in LF, we measured mRNA of PDGFRs in normal and scleroderma LF. We found that the amount of PDGFRα mRNA exceeds 5.27±1.6-fold the amount of PDGFRβ mRNA in SSc-ILD fibroblasts and 6.65±1.14-fold in normal LF (Fig. 1). This increase is statistically significant ($p<0.005$).

One of the early cellular events initiated by PDGF is a rapid, transient elevation in cytoplasmic Ca^{2+} (3). The ability of nintedanib to affect PDGF-induced intracellular Ca^{2+} was determined using a FLIPR cellular system. Acute increase of intracellular calcium was observed immediately upon PDGF administration in both control- and nintedanib-treated groups, without any significant difference in all studied cell lines.

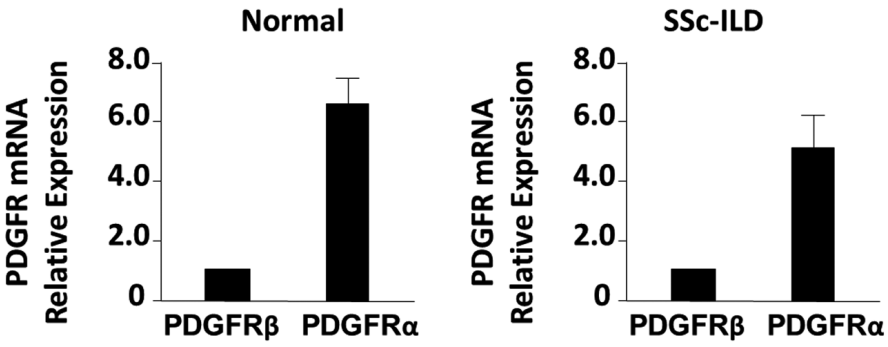

Fig. 1. Expression of PDGF receptors in normal and SSc-ILD LF. The PDGFRα expression is shown relative to the PDGFRβ.

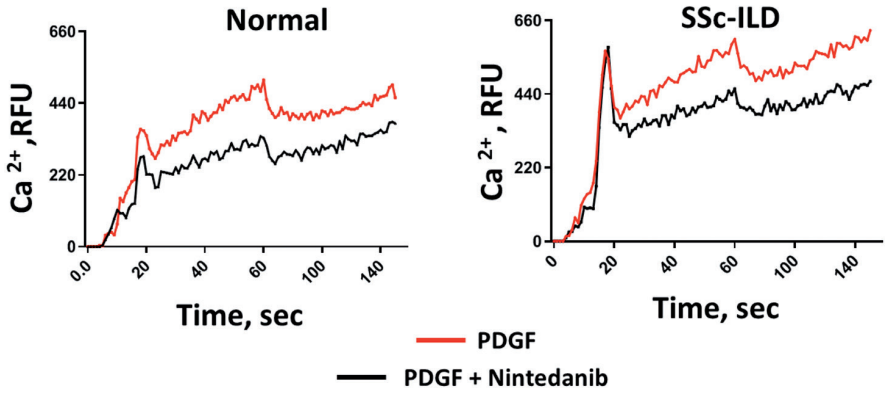

Fig. 2. Effect of nintedanib on PDGF-induced calcium efflux. Cells were challenged with PDGF-BB at t=0 sec and fluorescence signals were recorded to determine intracellular Ca^{2+} concentration. A representative recording for normal and SSc-ILD LF is depicted, respectively.

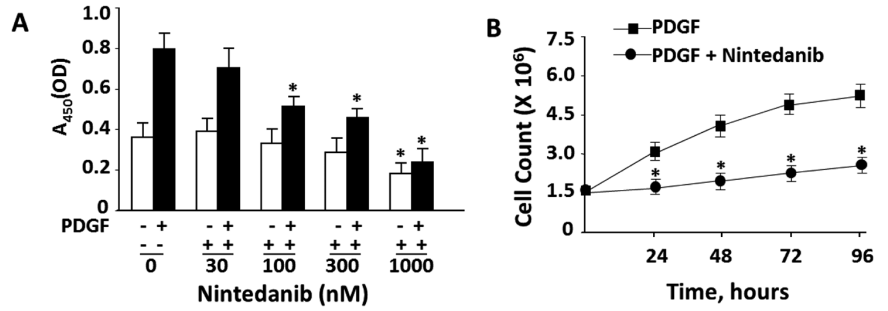

Fig. 3. Nintedanib inhibits PDGF-induced cell proliferation in a concentration-dependent and time-dependent manner. LF from patients with SSc-ILD were incubated with nintedanib at different concentrations and stimulated ± PDGF-BB and incubated for 24 h (**A**). PDGF-BB-stimulated cells were incubated ± nintedanib at 100 nM for up to 96 h (**B**). Data are presented as mean ± SD. The asterisk represents statistically significant differences ($p<0.05$) between cells treated with nintedanib *vs*. non-treated cells (**A**) or between cells stimulated with PDGF and nintedanib *vs*. cells only stimulated with PDGF (**B**).

However, the intracellular calcium in non-nintedanib treated cells maintained higher fluorescent levels in the presence of PDGF, which were significantly reduced ($p<0.0001$) in the nintedanib-treated group. A second peak represents a delayed calcium efflux which was observed at the 60 sec time point equal to 604.26±40.3 RFU in SSc and 511.5±77.26 RFU in normal LF. Nintedanib significantly ($p<0.0001$) reduced PDGF-induced delayed calcium efflux reducing its value at the 60 sec time point to 455.58±46.09 RFU and 334.3±36.24 RFU in SSc-ILD and control lung fibroblasts, respectively (Fig. 2).

Effect of nintedanib on lung fibroblast proliferation

We measured the effect of nintedanib on PDGF-induced LF proliferation using a quick cell proliferation assay. Basal OD unit levels of viable scleroderma LF cultured in serum-free medium (SFM) were in the range of 0.29 - 0.43 with an average of 0.37±0.05 OD. PDGF increased cell proliferation 2.1-fold within 24 hours (Fig. 3A). At concentrations of 30, 100, and 300 nM nintedanib had no significant effect on unstimulated SSc lung fibroblast proliferation. Only at a concentration of 1 μM, nintedanib significantly ($p<0.05$) reduced unstimulated SSc lung fibroblast proliferation from 0.37±0.05 OD to 0.2±0.04 OD. However, PDGF-induced cell proliferation was inhibited by nintedanib in a concentration-dependent manner, reaching statistical significance at 100 nM, 300 nM and 1μM (Fig. 3A).

Additionally, we measured time-dependent effects of nintedanib on PDGF-induced proliferation of SSc LF. Cells cultured in 1% FCS were stimulated with PDGF (40 ng/ml) with or without nintedanib (100 nM) for 24 h, 48 h, 72 h, and 96 h. LF incubated with 1% FCS were used as a control. The effect of 100 nM nintedanib alone was similar to that observed in control cells (data not shown). The proliferation rate of cells stimulated with PDGF was increased two-fold within 24 h and further increased 3.4-fold within 96 h. Nintedanib significantly ($p<0.01$) inhibited PDGF-induced proliferation of SSc LF at all-time points measured. The proliferation rate of cells stimulated with nintedanib and PDGF was reduced 1.9-fold within 24 h, 2.1-fold within 48 h, and 2.5-fold within 72 h and 96 h as compared to cells stimulated with PDGF alone (Fig. 3B).

Effect of nintedanib on LF migration

To study effects of nintedanib on migration of SSc-ILD fibroblasts we utilised a scratch assay that measures cell migration toward the injured sites. The migration rate of SSc-ILD fibroblasts in SFM was 38.2±7.9% in six hours. PDGF further increased the migration rate of SSc-ILD fibroblasts to 62.8±12.5%. Nintedanib decreased basal and PDGF-induced migration of SSc-ILD fibroblasts in a concentration-

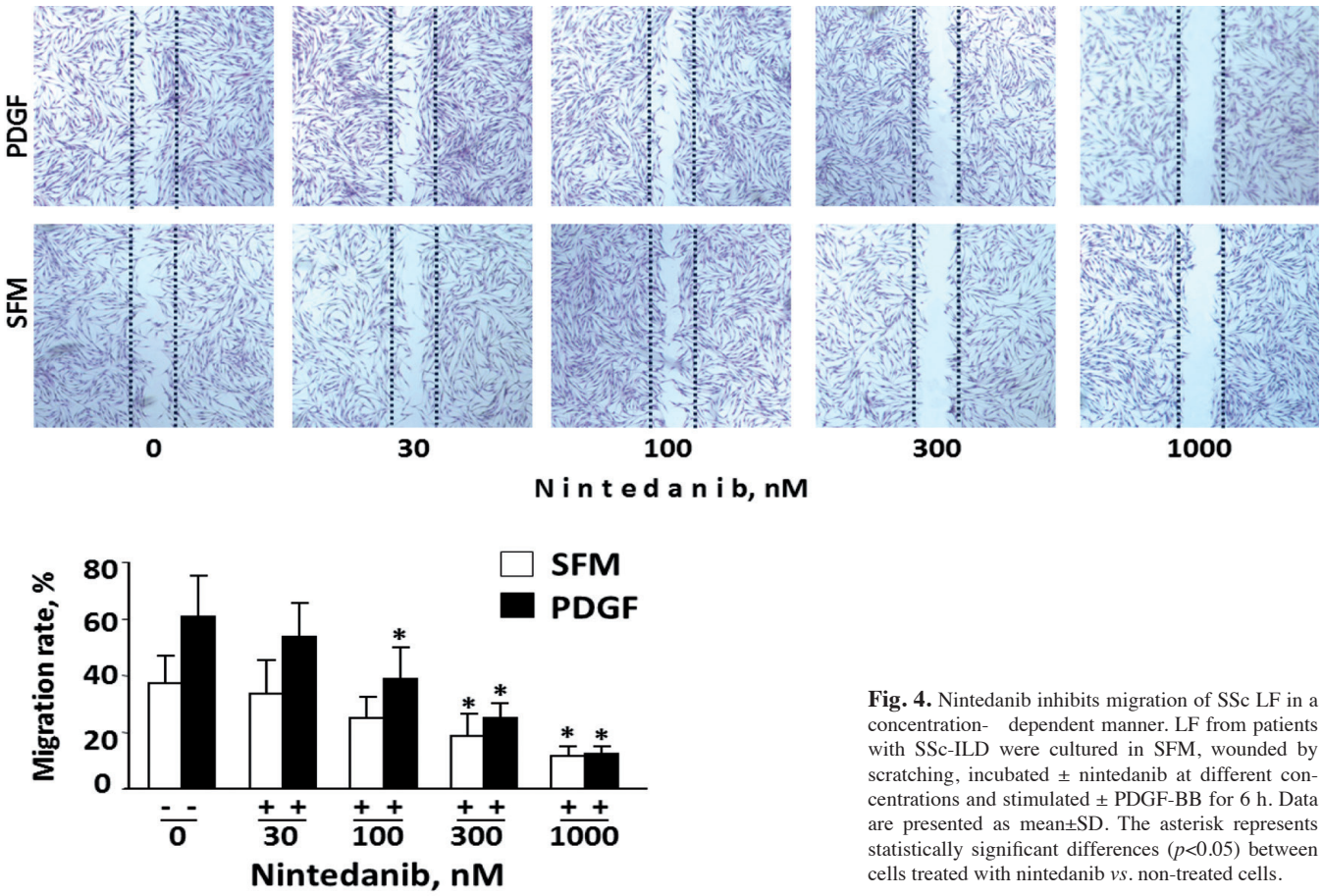

Fig. 4. Nintedanib inhibits migration of SSc LF in a concentration- dependent manner. LF from patients with SSc-ILD were cultured in SFM, wounded by scratching, incubated ± nintedanib at different concentrations and stimulated ± PDGF-BB for 6 h. Data are presented as mean±SD. The asterisk represents statistically significant differences (p<0.05) between cells treated with nintedanib *vs*. non-treated cells.

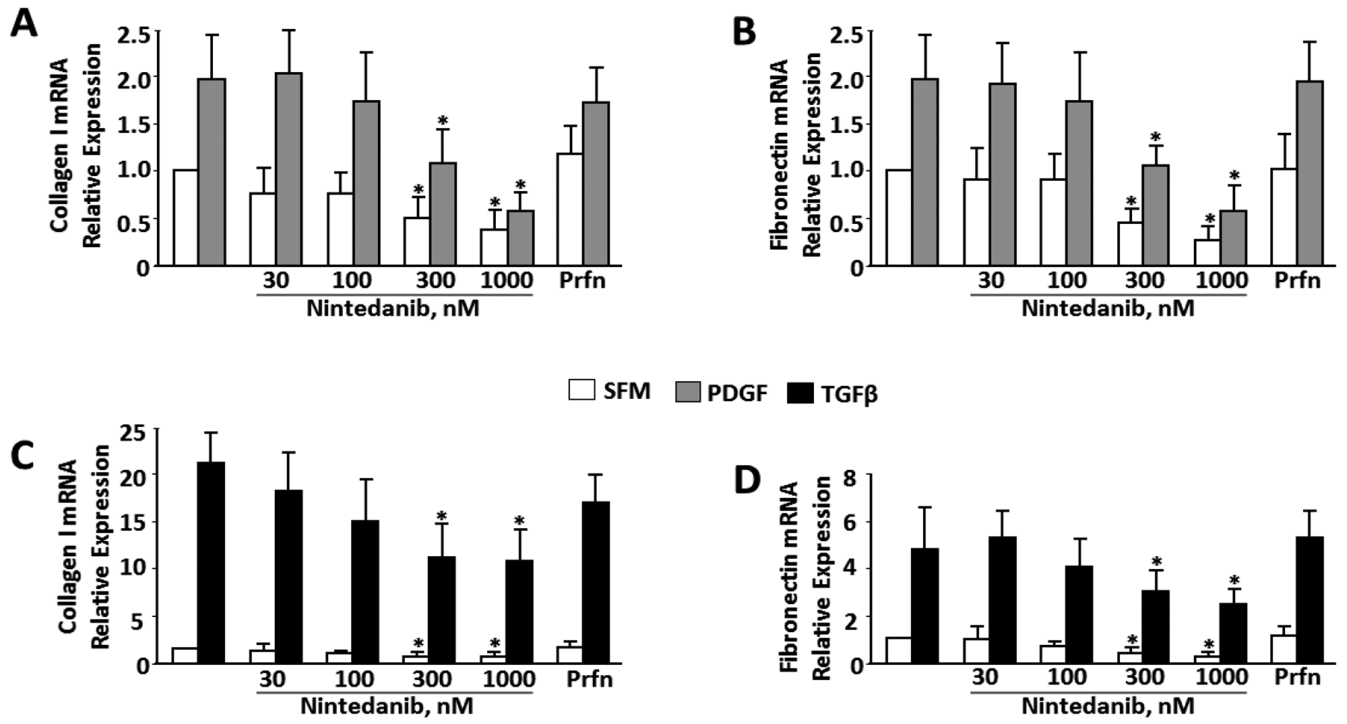

Fig. 5. Nintedanib reduces collagen type I mRNA and fibronectin mRNA expression in SSc LF in a concentration-dependent manner. LF from patients with SSc-ILD were cultured in SFM, incubated ± nintedanib at different concentrations or pirfenidone (Prfn) at 100 μM and stimulated ± PDGF-BB or TGFβ for 24 h. Data are presented as mean±SD. The asterisk represents statistically significant differences (p<0.05) between cells treated with nintedanib *vs*. non-treated cells.

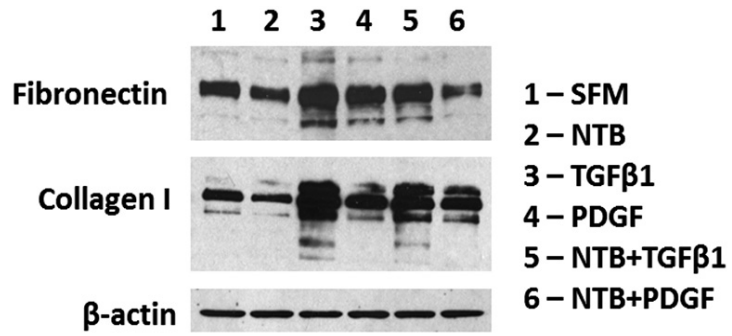

Fig. 6. Nintedanib reduces fibronectin and collagen type I proteins in SSc LF. LF from patients with SSc-ILD were cultured in serum free medium (SFM), incubated ± nintedanib (NTB) at different concentrations and stimulated ± PDGF-BB or TGFβ for 24 h. A representative immunoblot is presented.

dependent manner (Fig. 4). The migration rate in scleroderma LF incubated with 100 nM nintedanib was significantly (p<0.05) reduced to 39.1±9.0% in the presence of PDGF and to 26.6±7.2% in SFM (Fig. 4).

Effects of nintedanib on ECM proteins (collagen type I and fibronectin) in SSc-ILD fibroblasts

To establish whether nintedanib would interfere with the expression of the ECM proteins, we incubated scleroderma lung fibroblasts with nintedanib in the presence and absence of PDGF (40 ng/ml) or TGFβ (2.5 ng/ml) for 24 hours followed by measurement of mRNA levels of collagen type I and fibronectin. Nintedanib reduced basal levels and PDGF- and TGFβ-induced collagen type I and fibronectin mRNA in a concentration-dependent manner in SSc-ILD LF. However, in our study a statistically significant effect was not observed at a concentration of nintedanib below 300 nM (Fig. 5 A-D). Note that pirfenidone at a concentration of 100 μM had no effects on either collagen or fibronectin mRNA expression in SSc-ILD fibroblasts. Immunoblotting experiments further confirmed that nintedanib at a concentration of 300 nM reduces basal as well as TGFβ- and PDGF-induced protein levels of collagen type I and fibronectin expression in SSc-ILD LF (Fig. 6).

Effects of nintedanib on α-SMA in LF

SSc-ILD fibroblasts or myofibroblasts are characterised by expression of a contractile isoform of actin, α-SMA. To investigate the regulation of the α-SMA promoter in lung fibroblasts, we performed a luciferase reporter assay. We observed that PDGF increases transcriptional activity of α-SMA promoter 2.48±0.61-fold in normal lung fibroblasts (Fig. 7A) and 1.9±0.38-fold in SSc-ILD fibroblasts (Fig. 7B). Nintedanib at a concentration of 100 nM had no effect on basal levels of the α-SMA promoter, but significantly (p<0.05) reduced PDGF-induced transcriptional activity of α-SMA in nor-

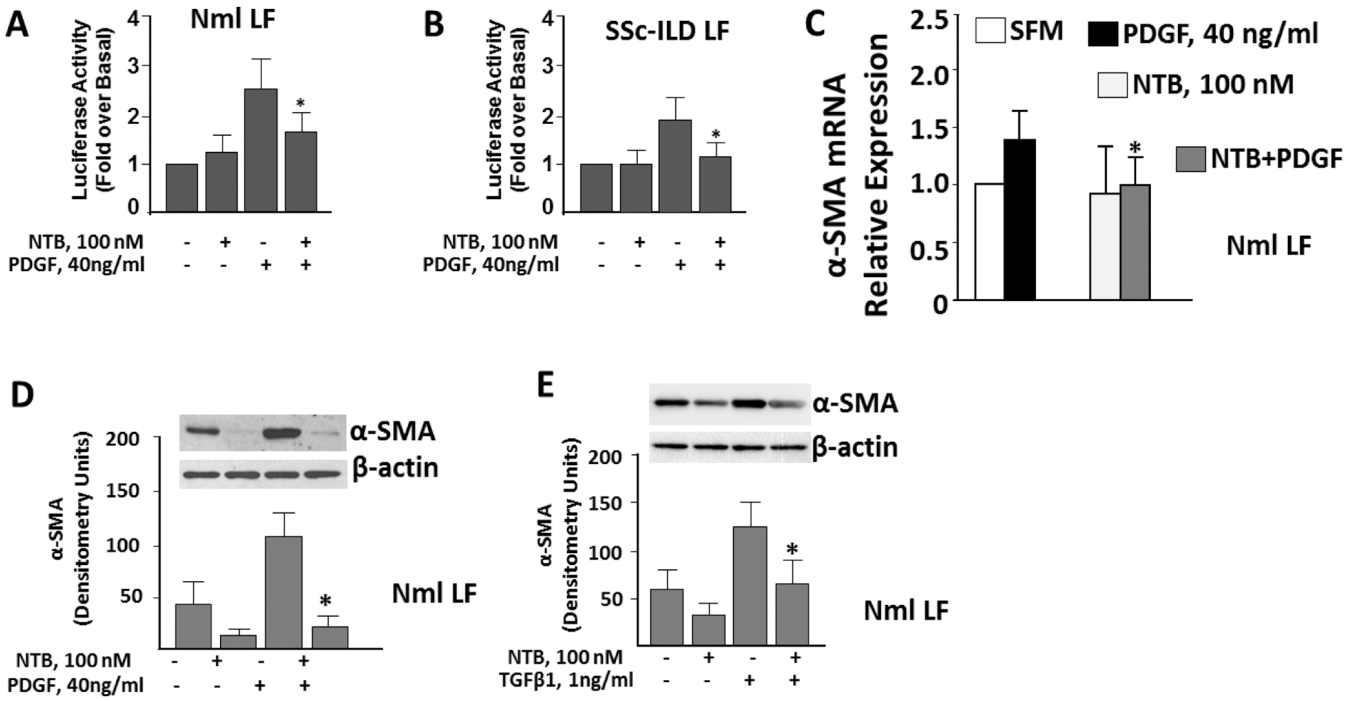

Fig. 7. Nintedanib attenuates α-SMA promoter activity, mRNA and protein expression in LF. LF were cultured in SFM, incubated ± nintedanib (NTB) at 100 nM and stimulated ± PDGF-BB (40 ng/ml) for 24 h or ± TGFβ (1 ng/ml) for 7 days. PDGF-induced α-SMA promoter activity was determined by luciferase assay in normal (Nml) LF (A) and in SSc-ILD LF (B). PDGF-induced relative α-SMA mRNA expression is depicted in (C) and protein expression in (D). TGFβ-induced α-SMA protein expression is presented in (E). Data are mean ± SD of three independent experiments. The asterisk represents statistically significant differences (p<0.05) between cells stimulated with PDGF or TGF and nintedanib *versus* cells treated with PDGF or TGF alone.

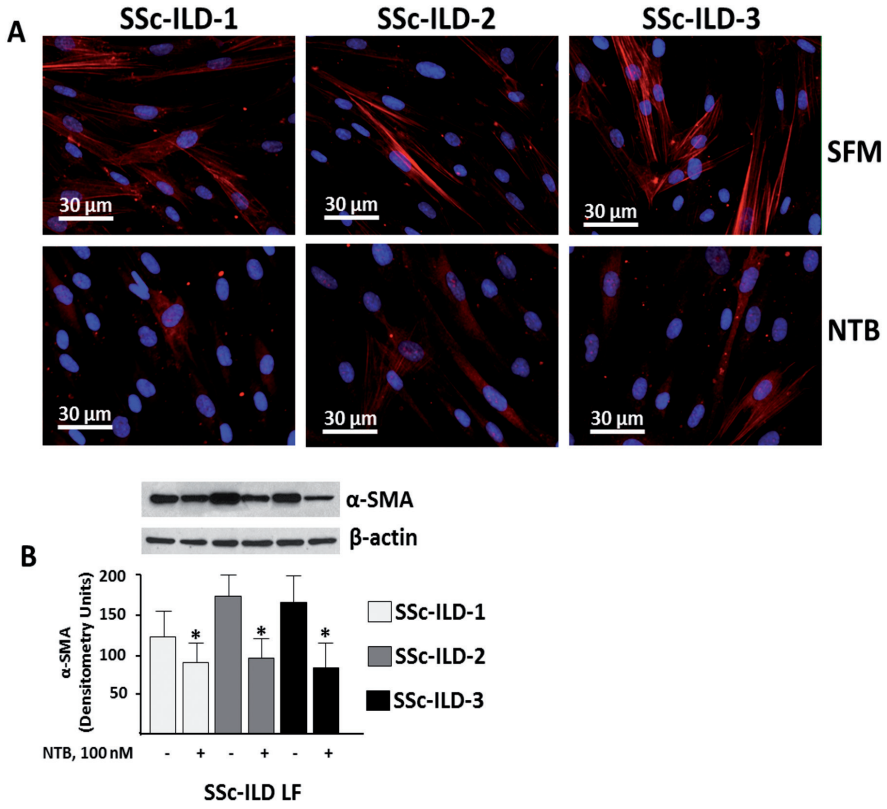

Fig. 8. Nintedanib inhibits α-SMA expression and organisation in SSc-ILD LF. LF from three different patients with SSc-ILD were cultured in SFM and incubated ± nintedanib (NTB) at 100 nM for 24 h. Representative immunohistochemistry slides from the different SSc-ILD cell lines show α-SMA staining in red and DAPI in blue (A). Representative immunoblots and densitometric analysis of immunoblots from 3 independent experiments are presented in (B). The asterisk represents statistically significant differences (p<0.05) between cells treated with nintedanib *vs*. untreated cells.

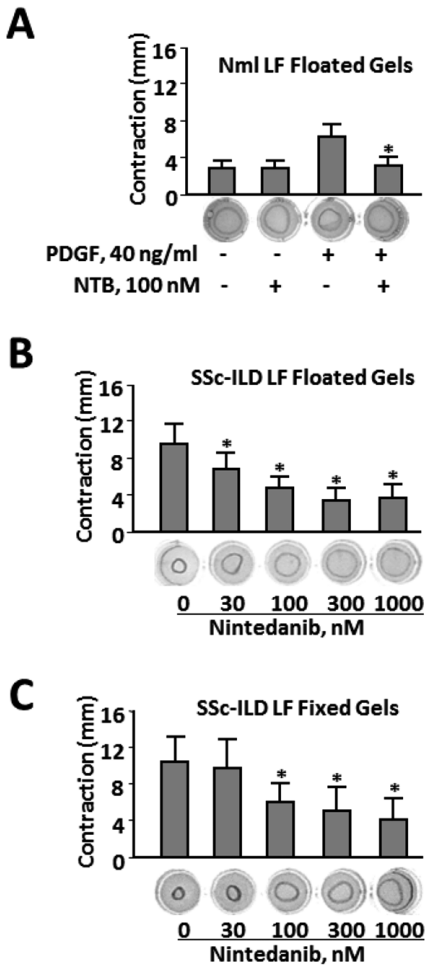

Fig. 9. Nintedanib inhibits contraction of collagen gels populated with LF in a concentration-dependent manner. Contraction of normal (Nml) LF embedded in a floating collagen matrix was stimulated with PDGF ± nintedanib (NTB) at 100 nM (**A**). SSc-ILD LF embedded in a floating collagen matrix (**B**) or a fixed matrix (**C**) contracted spontaneously. Nintedanib in a concentration-dependent manner significantly inhibited the contraction. Data are presented as mean±SD of three independent experiments. The asterisk represents statistically significant differences between cells stimulated with nintedanib *vs*. unstimulated cells (p<0.05).

mal (Fig. 7A) and SSc lung fibroblasts to 1.5±0.35-fold and 1.15±0.2-fold, respectively (Fig. 7B).

PDGF had no significant effect on α-SMA mRNA in SSc-ILD fibroblasts (data not shown), but increased the levels of α-SMA mRNA 1.41±0.25-fold over basal level in normal lung fibroblast (Fig. 7C). Nintedanib at a concentration of 100 nM significantly (p<0.05) decreased PDGF-induced α-SMA mRNA from 1.41±0.25-fold over basal level to 0.99±0.27-fold over basal level in normal lung fibroblasts. Similarly, nintedanib significantly (p<0.05) reduced PDGF-induced α-SMA protein from 100.1±31.1 densitometry units (DU) to 20.6±16.8 DU in normal lung fibroblasts (Fig. 7D).

To investigate effects of nintedanib on TGFβ-induced α-SMA, we cultured normal lung fibroblasts for 7 days in serum-free DMEM supplemented with or without nintedanib (100 nM) and TGFβ (1 ng/ml). Expression of α-SMA protein was studied by immunoblotting and consequent densitometry analysis. We observed that prolonged exposure of normal lung fibroblasts to low concentration of TGFβ results in 2.18-fold increase of α-SMA protein from 60.1±20.8 DU to 130.9±25.7 DU. Nintedanib significantly (p<0.05) decreased TGFβ-induced α-SMA protein reducing it to 66.8±27.2 DU (Fig. 7E).

Experiments using immunofluorescent staining further confirmed that PDGF had no significant effects on α-SMA in SSc-ILD fibroblasts (data not shown). However, nintedanib at a concentration of 100 nM reduced the expression and organisation of α-SMA in all studied SSc-ILD cell lines from 3 different donors (SSc-ILD-1, -2 and -3) (Fig. 8A). Immunoblotting experiments confirmed that 24-h exposure of nintedanib at a concentration of 100 nM leads to significant (p<0.05) reduction of α-SMA protein in SSc-ILD fibroblasts (Fig. 8B). Using densitometric analysis of α-SMA immunoblots, we found that nintedanib reduced α-SMA protein from 121.4±32.2 to 93.1±27.1 DU in SSc-ILD-1, from 164.6±28.2 to 97.7±25.7 DU in SSc-ILD-2, and from 156.0±41.8 to 82.3±29.4 DU in SSc-ILD-3 cell lines.

Effect of nintedanib on contraction of collagen gels populated with SSc-ILD and normal LF

PDGF induced significant (p<0.05) contraction of floating collagen gels populated with normal LF (from

2.92±0.83mm to 6.16±1.63mm, Fig. 9A). However, PDGF had no effects on fixed collagen gels populated with normal LF nor on either fixed or floated collagen gels populated with SSc-ILD LF. Nintedanib at concentration of 100 nM significantly (p<0.05) inhibited PDGF-induced contraction of floating collagen gels populated with normal LF from 6.16±1.63 mm to 3.03±1.17 mm.

Normal LF cultured either in fixed or floated collagen gels and incubated with nintedanib alone contracted to a similar extent as cells in SFM (data not shown). In contrast, SSc-ILD LF characterised by inherently high contractile activity constricted notably less in the presence of nintedanib. We observed that nintedanib decreases contractile activity of SSc-ILD LF in a concentration-dependent manner in both floated and fixed collagen gels. SSc-ILD fibroblasts cultured within floated collagen gels contracted those by 9.13±2.24 mm. A significant inhibition of floated collagen gel contraction by nintedanib was observed starting at 30 nM (6.43±1.81 mm, p<0.05), further reducing collagen gel contraction at concentrations of 100 nM (4.78±1.33 mm), 300 nM (3.73±1.55 mm), and 1 μM (3.9±1.64 mm) (Fig. 9B). Basal contractile activity of fixed collagen gels populated with SSc-ILD LF was 10.23±3.32 mm. Nintedanib reduced the contractile activity of SSc-ILD LF within fixed collagen gels starting at 100 nM (6.18±1.87 mm, p<0.05), demonstrating further activity at concentrations of 300 nM (5.13±2.24 mm), and at 1μM (4.02±1.91 mm) (Fig. 9C).

Discussion

Fibroblasts are one of the most abundant cells in fibrotic tissues. They play a critical role in SSc-ILD as well as in many other types of pulmonary fibrosis. Our laboratory and many others have demonstrated that fibroblasts isolated from fibrotic lesions retain their pro-fibrotic phenotype and can be used as a cellular model to study the antifibrotic mechanisms of newly developed pharmaceuticals (1, 15, 18). Herein we report antifibrotic effects of nintedanib in LF isolated from SSc-ILD patients.

Nintedanib is a potent intracellular inhibitor of several receptor tyrosine kinases including PDGFRs (7, 8), which abundantly occupy the surface of mesenchymal cells including fibroblasts (3, 17). We observed that control and SSc-ILD LF express significantly higher amount of PDGFRα mRNA as compared to PDGFRβ mRNA. Nintedanib has no effect on the expression of PDGFRs (data not shown), yet it significantly reduced PDGF-stimulated delayed calcium efflux. Quiescent cells maintain Ca^{2+} at relatively low levels through the activity of Ca^{2+} pumps on the plasma membrane or on the endoplasmic reticulum. In response to excitatory stimulation, Ca^{2+} is elevated by the opening of Ca^{2+}-permeable ion channels on those membranes. Ca^{2+} influx can contribute to the remodelling of cell-dense tissue by coordinating the activity of myofibroblasts (19). Mukherjee *et al*. demonstrated that calcium waves induced in human pulmonary fibroblasts either by TGFβ or PDGF markedly amplify the gene transcription of connective tissue matrix proteins (20, 21).

PDGF-induced Ca^{2+} influx can also contribute to cell migration (22). Cell migration is a fundamental cellular process for normal development and homeostasis of tissues and organs. Fibroblasts of normal stroma are relatively stationary despite the absence of architectural boundaries such as basement membranes. Pulmonary fibroblasts isolated from SSc-ILD patients are characterised by enhanced migratory capacity and, when cultured on fibronectin matrix, can be used as an *in vitro* model to study the migration of myofibroblasts to foci of lung fibrosis (23). Signalling through the PDGF/PDGFR axis is a key feature of enhanced migration (24). In agreement with this, our data demonstrate that SSc-ILD fibroblasts migrate faster in the presence of PDGF as compared to SFM without PDGF. Importantly, nintedanib effectively reduced basal and PDGF-induced migration of SSc-ILD fibroblasts in a concentration-dependent manner.

LF derived from SSc-ILD patients are characterised by increased proliferative capacity and by high expression of ECM proteins such as collagen type I and fibronectin (2, 25 - 27). PDGF is a major mitogen for mesenchymal cells and the strongest identified proliferative stimulus for fibroblasts (3-5, 24), whereas TGFβ is a major inducer of α-SMA and ECM genes and proteins in scleroderma fibroblasts (26, 28). Here we demonstrate that nintedanib inhibits the proliferation of SSc-ILD LF in both concentration- and time-dependent manners. Additionally, we show that nintedanib downregulates collagen and fibronectin in scleroderma LF and inhibits α-SMA protein induced in normal lung fibroblasts by prolonged exposure to low concentrations of TGFβ.

Activated LF, or myofibroblasts, isolated from SSc patients retain their pro-fibrotic phenotype for several passages in cell culture (1, 2) and when cultured in collagen gel matrices, can be used as a model system for understanding the nature of persistent fibrosis in scleroderma. Contraction of floating collagen gels is considered to resemble more closely the initial phase of fibrosis and reflects the induction of the myofibroblast phenotype by various growth factors (18, 29). In contrast, attached or fixed collagen gels serve as a model of the late phase of excessive scarring and reflect the direct ability of proteins to enhance contraction of already formed α-SMA fibers through mechanical stress (18, 29). We observed that PDGF had no effect on either fixed or floated collagen gels populated with SSc-ILD LF. However, nintedanib reduced basal contractile activity of SSc-ILD LF in a concentration-dependent manner in both floating and fixed collagen gels. Similarly, nintedanib significantly reduced expression and organisation of α-SMA in SSc-ILD LF.

We speculate that the profound effect of nintedanib on contractile activity of SSc-ILD fibroblasts might be explained by the direct interference of nintedanib with α-SMA protein. Monomeric or globular (G-actin) α-SMA, like any other actin, exists in cells in ATP-bound forms (30). SSc-ILD fibroblasts coordinate the formation of α-SMA filament (F-actin) networks from a general cytoplasmic pool of monomeric α-SMA at the correct time and place to regulate crucial cellular events such as motility or contractility. The initiation of

α-SMA polymerisation or organisation in stress fibers is primarily controlled by signalling pathways of various profibrotic growth factors, including PDGF (2, 31, 32), or by mechanical stress (33). The polymerisation itself occurs by addition of ATP-bound G-actin to the dynamic barbed end of a forming filament (30). We hypothesise that nintedanib might directly interfere with α-SMA-ATP-bound pocket affecting α-SMA interaction with actin-binding proteins and generation of contractile forces. Alternatively, nintedanib could induce degradation of α-SMA in scleroderma lung myofibroblasts similar to staurosporine-induced cleavage of α-SMA in myofibroblasts reported by Nakazono-Kusaba *et al*. (34). Further studies clarifying regulation of α-SMA by nintedanib in lung myofibroblasts will be necessary.

To our knowledge this is the first work to investigate effects of nintedanib on LF isolated from SSc-ILD patients. The effectiveness of nintedanib in SSc LF in our study is comparable to antifibrotic efficacy of this drug in SSc skin fibroblasts (13) and in LF from patients with IPF published by others (9-12). Our data demonstrate that nintedanib at a concentration as low as 100 nM inhibits proliferation, migration, and ECM protein in SSc LF. Additionally, our data suggest that nintedanib might be more effective in SSc lung myofibroblasts as compared to IPF lung myofibroblasts. In the current study, we show that nintedanib reduces α-SMA protein in SSc lung myofibroblasts at a concentration of 100 nM, while previously published studies by others in IPF lung myofibroblasts showed α-SMA inhibition by nintedanib at much higher concentrations (10, 11). The concentration of 100 nM is especially important as it is within the range of the clinical exposure of nintedanib. The Cmax determined in patients in clinical studies after steady-state standard dosing of nintedanib at 150 mg bid is 59 - 74 nmol/L (35-37). Antifibrotic effects of nintedanib in SSc LF at the clinically relevant concentrations suggest efficacy of nintedanib in scleroderma patients and further advocates this drug as a potentially effective antifibrotic treatment against SSc-ILD.

Acknowledgements

The authors would like to thank the MUSC MCRC (NIH/NIAMS P60 AR062755) for lung fibroblasts and Dr M.L. Lee at the MUSC FLIPR^{TETRA} Core S10 RR02777 for assistance with the Calcium study.

References

1. LEROY EC: Increased collagen synthesis by scleroderma skin fibroblasts *in vitro*. A possible defect in regulation or activation of scleroderma fibroblasts. *J Clin Invest* 1974; 54: 880-9.
2. BOGATKEVICH GS, TOURKINA E, SILVER RM, LUDWICKA-BRADLEY A: Thrombin differentiates normal lung fibroblasts to a myofibroblast phenotype via the proteolytically activated receptor-1 and a protein kinase C-dependent pathway. *J Biol Chem* 2001; 276: 45184-92.
3. ANDRAE J, GALLINI R, BETSHOLTZ C: Role of platelet-derived growth factors in physiology and medicine. *Genes Dev* 2008; 22: 1276-312.
4. VIGNAUD JM, ALLAM M, MARTINET N, PECH M, PLENAT F, MARTINET Y: Presence of platelet-derived growth factor in normal and fibrotic lung is specifically associated with interstitial macrophages, while both interstitial macrophages and alveolar epithelial cells express the c-sis proto-oncogene. *Am J Respir Cell Mol Biol* 1991; 5: 531-8.
5. ANTONIADES HN, BRAVO MA, AVILA RE *et al*.: Platelet-derived growth factor in idiopathic pulmonary fibrosis. *J Clin Invest* 1990; 86: 1055-64.
6. LUDWICKA A, OHBA T, TROJANOWSKA M *et al*.: Elevated levels of platelet derived growth factor and transforming growth factor-beta 1 in bronchoalveolar lavage fluid from patients with scleroderma. *J Rheumatol* 1995; 22: 1876-83.
7. ROTH GJ, HECKEL A, COLBATZKY F *et al*.: Design, synthesis, and evaluation of indolinones as triple angiokinase inhibitors and the discovery of a highly specific 6-methoxycarbonyl-substituted indolinone (BIBF 1120). *J Med Chem* 2009; 52: 4466-80.
8. WOLLIN L, MAILLET I, QUESNIAUX V *et al*.: Antifibrotic and anti-inflammatory activity of the tyrosine kinase inhibitor nintedanib in experimental models of lung fibrosis. *J Pharmacol Exp Ther* 2014; 349: 209-20.
9. HOSTETTLER KE, ZHONG J, PAPAKONSTANTINOU E *et al*.: Anti-fibrotic effects of nintedanib in lung fibroblasts derived from patients with idiopathic pulmonary fibrosis. *Respir Res* 2014; 15: 157.
10. LEHTONEN ST, VEIJOLA A, KARVONEN H *et al*.: Pirfenidone and nintedanib modulate properties of fibroblasts and myofibroblasts in idiopathic pulmonary fibrosis. *Respir Res* 2016; 17: 14.
11. RANGARAJAN S, KURUNDKAR A, KURUNDKAR D *et al*.: Novel Mechanisms for the Antifibrotic Action of Nintedanib. *Am J Respir Cell Mol Biol* 2016; 54: 51-9.
12. KNUPPEL L, ISHIKAWA Y, AICHLER M *et al*.: A novel antifibrotic mechanism of nintedanib and pirfenidone. inhibition of collagen fibril assembly. *Am J Respir Cell Mol Biol* 2017; 57: 77-90.
13. HUANG J, BEYER C, PALUMBO-ZERR K *et al*.: Nintedanib inhibits fibroblast activation and ameliorates fibrosis in preclinical models of systemic sclerosis. *Ann Rheum Dis* 2016; 75: 883-90.
14. VAN DEN HOOGEN F, KHANNA D, FRANSEN J *et al*.: 2013 classification criteria for systemic sclerosis: an American College of Rheumatology/European League against Rheumatism collaborative initiative. *Arthritis Rheum* 2013; 65: 2737-47.
15. ATANELISHVILI I, SHIRAI Y, AKTER T *et al*.: M10, a caspase cleavage product of the hepatocyte growth factor receptor, interacts with Smad2 and demonstrates antifibrotic properties *in vitro* and *in vivo*. *Transl Res* 2016; 170: 99-111.
16. PFAFFL MW: A new mathematical model for relative quantification in real-time RT–PCR. *Nucl Acids Res* 2001; 29: 2002-7.
17. DONOVAN J, SHIWEN X, ABRAHAM D: Platelet-derived growth factor alpha and beta receptors have overlapping functional activities towards fibroblasts. *Fibrogenesis Tissue Repair* 2013; 6: 10.
18. BOGATKEVICH GS, SILVER RM: Dabigatran, a direct thrombin inhibitor, demonstrates anti-fibrotic effects on lung fibroblasts. *Arthritis Rheum 2009;* 60: 3455-3464.
19. FOLLONIER L, SCHAUB S, MEISTER JJ, HINZ B: Myofibroblast communication is controlled by intercellular mechanical coupling. *J Cell Sci* 2008; 121(Pt 20): 3305-16.
20. MUKHERJEE S, KOLB MR, DUAN F, JANSSEN LJ: Transforming growth factor-β evokes Ca2+ waves and enhances gene expression in human pulmonary fibroblasts. *Am J Respir Cell Mol Biol* 2012; 46: 757-64.
21. MUKHERJEE S, DUAN F, KOLB MR, JANSSEN LJ: Platelet derived growth factor-evoked Ca2+ wave and matrix gene expression through phospholipase C in human pulmonary fibroblast. *Int J Biochem Cell Biol* 2013; 45: 1516-24.
22. YANG S, HUANG XY: Ca2+ influx through L-type Ca2+ channels controls the trailing tail contraction in growth factor-induced fibroblast cell migration. *J Biol Chem* 2005; 280: 27130-7.
23. BOGATKEVICH GS, LUDWICKA-BRADLEY A, SINGLETON CB, BETHARD JR, SILVER RM: Proteomic analysis of CTGF-activated lung fibroblasts: identification of IQGAP1 as a key player in lung fibroblast migration. *Am J Physiol Lung Cell Mol Physiol* 2008; 295: L603-11.
24. ALVAREZ RH, KANTARJIAN HM, CORTES JE: Biology of platelet-derived growth factor and its involvement in disease. *Mayo Clin Proc* 2006; 81: 1241-57.
25. LUDWICKA-BRADLEY A, BOGATKEVICH GS, SILVER RM: Thrombin-mediated cellular events in pulmonary fibrosis associated with systemic sclerosis (scleroderma). *Clin Exp Rheumatol* 2004; 22 (Suppl. 33): S38-S46.
26. AKTER T, SILVER RM, BOGATKEVICH GS: Recent advances in understanding the pathogenesis of scleroderma-interstitial lung dis-

ease. *Curr Rheumatol Rep* 2014; 16: 411.
27. SHI-WEN X, RENZONI EA, KENNEDY L *et al*.: Endogenous endothelin-1 signaling contributes to type I collagen and CCN2 overexpression in fibrotic fibroblasts. *Matrix Biol* 2007; 26: 625-32.
28. VARGA J, WHITFIELD ML: Transforming growth factor-beta in systemic sclerosis (scleroderma). *Front Biosci* 2009; 1: 226-35.
29. GRINNELL F: Signal transduction pathways activated during fibroblast contraction of collagen matrices. *Curr Top Pathol* 1999; 93: 61-73.
30. ODA T, IWASA M, AIHARA T, MAEDA Y, NARITA A: The nature of the globular- to fibrous-actin transition. *Nature* 2009; 457: 441-45.
31. BOGATKEVICH GS, TOURKINA E, ABRAMS CS, HARLEY RA, SILVER RM, LUDWICKA-BRADLEY A: Contractile activity and smooth muscle-α actin organization in thrombin-induced human lung fibroblasts. *Am J Physiol Lung Cell Mol Physiol* 2003; 285: L334-L343.
32. LEASK A: Towards an anti-fibrotic therapy for scleroderma: targeting myofibroblast differentiation and recruitment. *Fibrogenesis Tissue Repair* 2010; 3: 8.
33. HINZ B, MASTRANGEO D, ISELIN CE, CHAPONNIER C, GABBIANI G: Mechanical tension controls granulation tissue contractile activity and myofibroblast differentiation. *Am J Pathol* 2001; 159: 1009-20.
34. NAKAZONO-KUSABA A, TAKAHASHI-YANAGA F, MORIMOTO S, FURUE M, SASAGURI T: Staurosporine-induced cleavage of alpha-smooth muscle actin during myofibroblast apoptosis. *J Invest Dermatol* 2002; 119: 1008-13.
35. SCHMID U, DOEGE C, DALLINGER C, FREIWALD M: Population pharmacokinetics of nintedanib in patients with idiopathic pulmonary fibrosis. *Pulm Pharmacol Ther* 2018; 48: 136-43.
36. MROSS K, STEFANIC M, GMEHLING D *et al*.: Phase I study of the angiogenesis inhibitor BIBF 1120 in patients with advanced solid tumors. *Clin Cancer Res* 2010; 16: 311-9.
37. EISEN T, SHPARYK Y, MACLEOD N *et al*.: Effect of small angiokinase inhibitor nintedanib (BIBF 1120) on QT interval in patients with previously untreated, advanced renal cell cancer in an open-label, phase II study. *Invest New Drugs* 2013; 31: 1283-93.